Journal of Applied Polymer Science

A versatile radiochromic dosimeter for low-medium gamma radiation and its application to food irradiation

Franceline Aparecida Lopes,[1,2] Giovana Ribeiro Ferreira,[1,3] Marcella Rocha Franco,[1] Thiago Schimitberger,[4] Luiz Oliveira de Faria,[4,5] Rodrigo Fernando Bianchi[1]

[1]Universidade Federal de Ouro Preto-UFOP, 35400-000 Ouro Preto MG, Brasil
[2]Universidade Federal de Viçosa, UFV-Campus Florestal, 35690-000 Florestal MG, Brasil
[3]Universidade Federal dos Vales do Jequitinhonha e Mucuri-UFVJM, 39440-000 Janaúba MG, Brasil
[4]Universidade Federal de Minas Gerais-UFMG, 31270-901 Belo Horizonte MG, Brasil
[5]Centro de Desenvolvimento da Tecnologia Nuclear-CDTN, 30161-970 Belo Horizonte MG, Brasil
Correspondence to: R. F. Bianchi (E-mail: bianchi@iceb.ufop.br)

ABSTRACT: This article presents a novel radiochromic film for selective detection of low-medium (0–10 kGy) gamma radiation (^{60}Co) doses. This dosimeter is based on a printed fluorescent multilayer structure comprising a paper substrate having layers of copper phthalocyanine (DY220) (a green emitter material) on the bottom, and layers of poly[2-methoxy-5(2′-ethylhexyloxy)-*p*-phenylenevinylene] (MEH-PPV) (a green-light absorber, red emitter, and radiation sensitive polymer) on the top. The effect of gamma radiation on the optical properties of DY220/MEH-PPV was described: it was observed as a strong correlation between radiation dose and fluorescent, color coordinates for CIE (1931) chromatic diagram, and Pantone color reference of the dosimeter. The rate of these changes can be altered by manipulation of top–bottom layers to represent easily the radiation dose to be determined in a wide range. This versatile dosimeter has many uses in the field of food radiation for monitoring, quality assurance, and control of the gamma radiation process. © 2017 Wiley Periodicals, Inc. J. Appl. Polym. Sci. **2018**, *135*, 45729.

KEYWORDS: conducting polymers; degradation; optical properties; sensors and actuators

Received 18 July 2016; accepted 12 November 2016
DOI: 10.1002/app.45729

INTRODUCTION

The extension of shelf life is the main objective of the food irradiation process. This method has received worldwide attention not only due to large post-harvest losses and the increasing concern about foodborne diseases, but also to the increase in the international trade of food products and strict export regulations.[1] This procedure is regulated by the Food and Drug Administration and has established safety standards for any food irradiated up to an overall average dose of 10 kGy.[2] It involves passing food through an ionizing radiation field (^{60}Co, ^{137}Cs, high-energy electrons, or X-ray)[3] that can penetrate fruit and vegetables and kill microorganisms, preventing food poisoning and spoilage without significantly raising the temperature of the food.[4,5] However, a reliable, quick, and easily operated dosimetry system is necessary for both process validation and control.[6,7]

In order to meet the requirements in the radiation processing, several dosimeters have been successfully developed and used as routine dosimetry systems for radiation processing, that is, various types of radiochromic plastic films,[8–17] GafChromic Dosimetry Media,[18–22] and aqueous solutions.[6,23–27] Particularly, radiochromic films have been extensively used for dosimetry in radiation medicine.[28,29] Their high spatial resolution is far superior to that of ionization chambers and thermoluminescent dosimeters, offering greater X-ray sensitivity and the ability to be used in water without waterproof encapsulation.[30] The energy response of multiple film types, such as "EBT" and "XR" series, has been studied by several authors.[31,32]

Although these devices have been extensively reported in the literature, conjugated polymers, especially poly[2-methoxy-5(2′-ethylhexyloxy)-*p*-phenylenevinylene] (MEH-PPV), a light-emitting polymer, have been highlighted as a very promising material for real-time solution-based dosimeters, due to the effects of radiation on the optical properties of MEH-PPV systems.[33–39] In general, MEH-PPV-based dosimeters may have explored the radiation effect on the overlap between the emission spectrum of a light-stable green emitter organic crystal [tris-(8-hydroxyquinoline)aluminum)] and the absorption spectrum of MEH-PPV solutions, to yield an optically integrated and multifunctional material. The basic idea behind this concept considers this

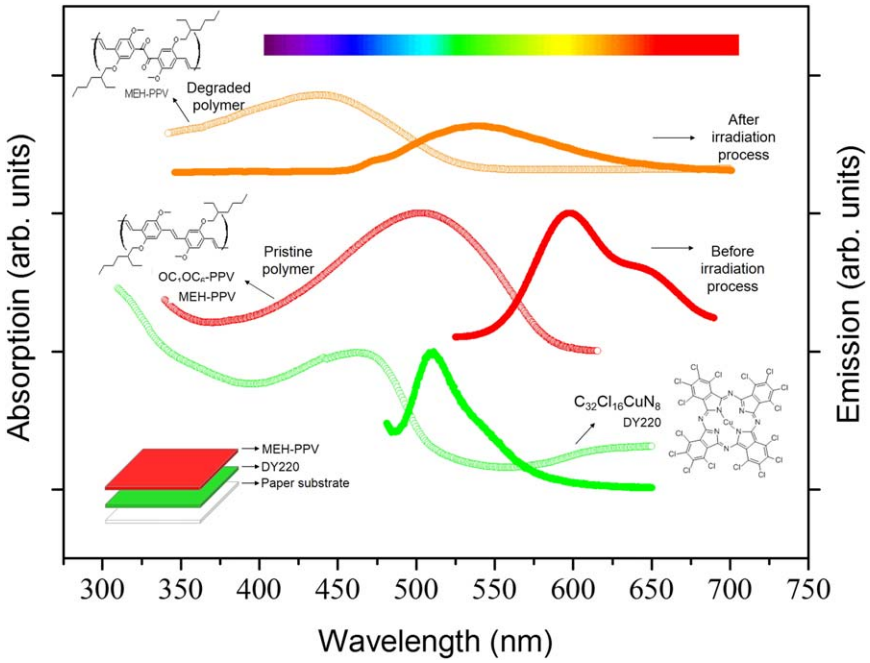

Figure 1. Absorption and photoemission spectra obtained from pristine MEH-PPV (OC1OC6-PPV), degraded MEH-PPV[40], and DY220 ($C_{32}Cl_{16}CuN_8$). The visible electromagnetic spectrum shown on top of the graph is intended to be used as a reference. The bottom-left scheme illustrates the general structure of the radiochromic multilayer organic dosimeter on paper-based substrate. [Color figure can be viewed at wileyonlinelibrary.com]

composite material as a luminescent *traffic-light* dosimeter, that is, a smart dosimeter, where red represents an underdose and green standing for the prescribed dose or overdose, while orange-yellow suggests that the radiation process is ongoing. However, some major drawbacks to adopting this system are related to the use of the toxic-chloroform-based dosimeter and to the green color evaluation of the MEH-PPV/Alq_3 system under white light. These disadvantages may cause harmful effects to humans, making it difficult for easy monitoring through the naked eye. This article seeks to address how to solve these problems.

In our study, the dosimeter consists of a multilayered film structure based on MEH-PPV and a green copper phthalocyanine pigment suitable for rotogravure inks. With this in mind, this study reports the development, characterization and performance evaluation of a novel, easy-to-read, and real-time printed radiochromic dosimeter for selective detection of low-medium (0–10 kGy) gamma radiation (^{60}Co) doses, and to satisfy regulatory requirements and quality assurance in food irradiation processes over a wide dose range.

EXPERIMENTAL

The radiochromic dosimeter is based on a multilayer structure comprising a multi-purpose white office paper (75 g m^{-2}) as substrate, copper phthalocyanine-$C_{32}Cl_{16}CuN_8$ (DY220), and MEH-PPV-OC_1OC_6-PPV. The copper phthalocyanine was obtained from Dyelux Indústria e Comércio LTDA (Brazil) and MEH from Aldrich-Sigma (Germany). All materials were used as received, without further purification and cleaning.

Radiochromic Film Dosimeter for Gamma Radiation (1.33 MeV, 0–10 kGy Range)

Figure 1 shows the device structure (bottom-left structure) and the large spectral overlap between DY220 emission and the absorption of both pristine and photodegraded MEH-PPV, which alters not only the color, but also the photoemission of the multilayer DY220:MEH-PPV film from red (before gamma irradiation process) to green (after gamma irradiation process). It is important to note that the optical overlap between DY220 and degraded MEH-PPV decreases and tends to disappear after radiation exposure.

This device is comprised of DY220 layers (1–10) on a white paper substrate covered by MEH-PPV layer (1–4). In order to print the layers, solutions were prepared by dissolving DY220 (10 g L^{-1}) in isopropyl alcohol, while MEH-PPV (1 g L^{-1}) in 70 vol % chloroform and 30 vol % isopropyl alcohol was present to reduce the evaporation rate during the printing process. The multilayer films were printed on multiple steps, one layer at a time, by means of rotogravure technique on paper substrate at 300 K, which is above the glass transition (T_g) of MEH-PPV,[41] to produce DY220:MEH-PPV multilayer films with a well-defined and reproducible thermal history. The rotogravure printer used was the G1 printability tester from GT Testing Systems Inc. The angle between the doctor blade and the printing cylinder was fixed at 60° with a pressure of approximately 6–7 N for this printing system. The printing cylinders used here have a line density of 70 lines cm^{-1}, 53° screen angle and 140° stylus angle with a 33-μm cell depth. A printing force of 200 N and printing speed of 0.6 m/s were used. The multilayer films were dried at room temperature overnight in the dark before being submitted to the cutting process. Rectangular shaped dosimeters with dimensions of (5 × 6) mm^2 were obtained and were stored at room temperature. Finally, the dosimeters were protected from light to avoid both photo and thermal degradation processes.

Gamma Radiation Procedure and Dosimeter Characterization

The irradiation of the device was performed at the Gamma Radiation Laboratory (LIG) within the Center for Development

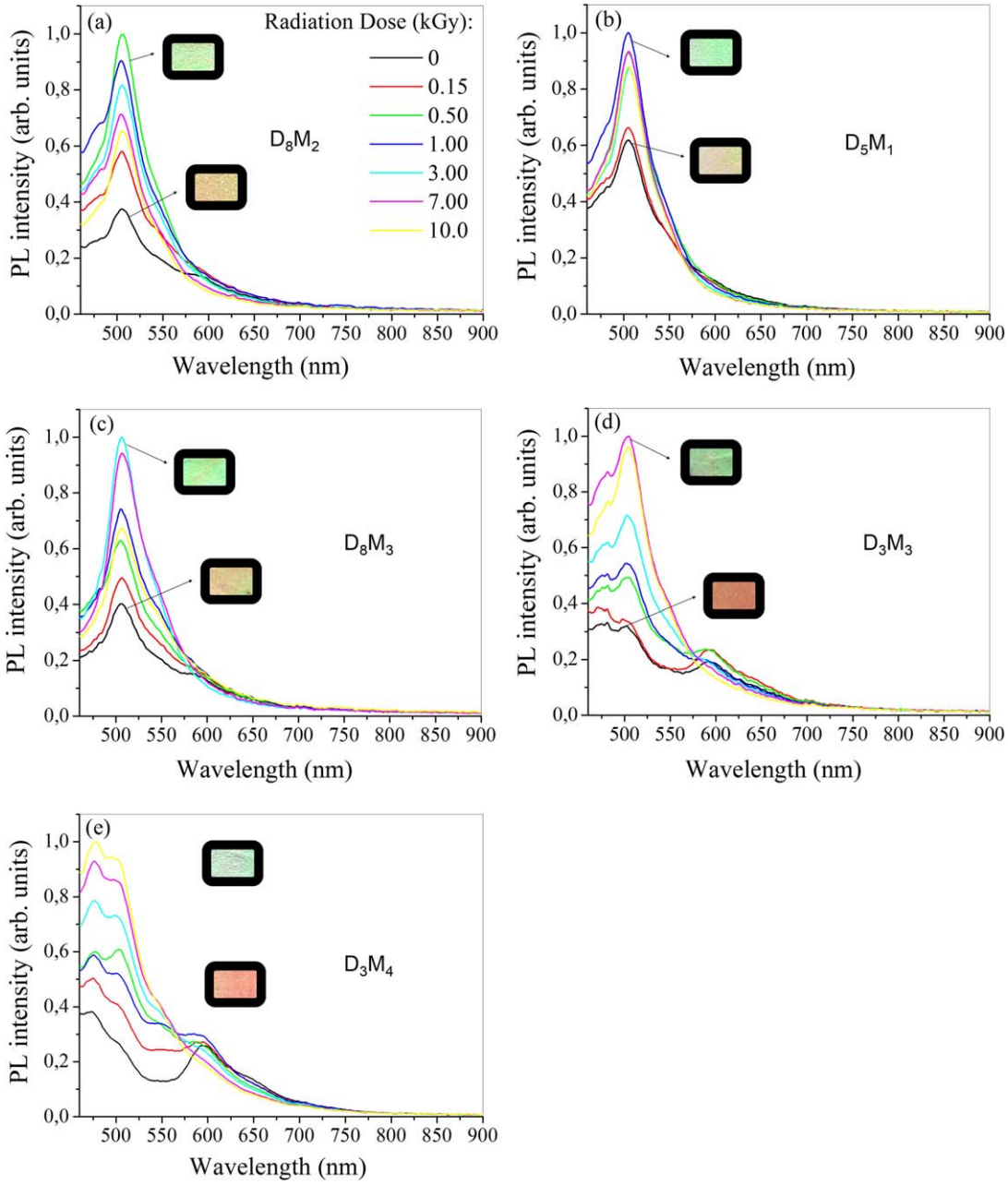

Figure 2. Photoluminescence spectrum of the dosimeters obtained from different DY220:MEH-PPV multilayer films (a) D8M2, (b) D5M1, (c) D8M3, (d) D3M3, and (e) D5M4 exposed to gamma radiation doses equal to 0, 0.15, 0.50, 1.00, 3.00, 7.00, and 10.00 kGy. Pictures of the devices before and after the irradiation process are shown as insets in the graphs. [Color figure can be viewed at wileyonlinelibrary.com]

of Nuclear Technology (CDTN). The gamma irradiation facility used in this study consists of a category II multipurpose panoramic irradiator (dry storage), model IR-214, type GB-127 (MDS Nordion, Canada), with a Cobalt-60 source and maximum radioactive activity of 2200 TBq or 60,000 Ci and 1.33 MeV. The radiation doses used were 0.15, 0.50, 1.00, 3.00, 7.00, and 10.00 kGy, doses considered useful in food irradiation processes,[5,42–44] under a dose rate of 20.00 kGy h^{-1}. In order to evaluate the effect of ionizing radiation on the optical properties of the films, a non-irradiated film (0 kGy) was used as a reference. The photoemission (PL) spectra of the DY220:MEH-PPV multilayer films were recorded using a USB2000 Ocean Optics spectrophotometer, with a violet LED (peak at approximately 415 nm, 400 mcd) as the excitation source. CIE (1931) chromaticity diagram color coordinates were obtained using the PL spectra of organic films and the Color Calculator Free Software. Finally, the color of the dosimeter was evaluated using a Pantone Color palette. All measurements were performed in the dark and at room temperature to prevent photo and thermal degradation processes.

RESULTS AND DISCUSSION

In order to evaluate the optical characteristics of the radiochromic DY220:MEH-PPV dosimeter, this system was exposed to

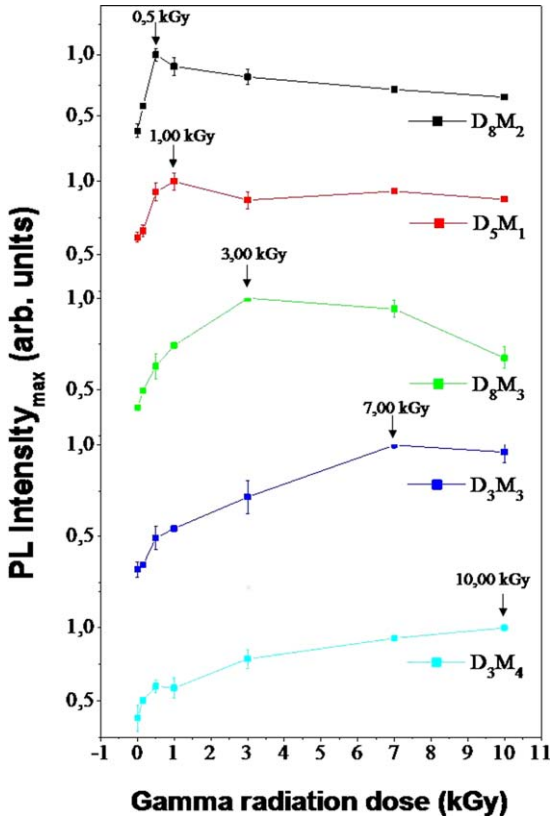

Figure 3. PL intensity at the maximum peak emission wavelength (λ_{max}) from DY220:MEH-PPV multilayer films obtained from the spectra from Figure 2 as a function of the gamma radiation dose. The arrows indicate the specific radiation dose described in the text. [Color figure can be viewed at wileyonlinelibrary.com]

radiation from 0 to 10 KGy. However, the results here are from the dosimeter that showed a color change after a particular dose of gamma radiation: 0.50, 1.00, 3.00, 7.00, and 10.00 kGy. These doses are useful in some food irradiation processes, such as insect disinfestations, parasite disinfestations, shelf-life extension, elimination of non-spore forming pathogenic bacteria, and reduction of microbial population in dry food ingredients.[5,42–44] In order to ease the discussion of the results, the following nomenclature was adopted: $D_{LG}M_{LR}$, where "LG" is the number of DY220 layers (i.e., green layers) and "LR", on the other hand, the number of MEH-PPV layers (red layers). For example, D_8M_2 is the device with eight DY220 layers and two MEH-PPV layers.

PL spectra of the DY220:MEH-PPV multilayer films exposed to gamma radiation are shown in Figure 2. Mean values from triplicate experiments are used. It should be noted that before the irradiation process, the D_8M_2, D_8M_3, D_3M_3, and D_3M_4 devices presented two bands, one with a peak centered around 505 nm (green emission) and another one centered around 595 nm (red-orange emission). In the D_5M_1 device, it is possible to observe only one band with a peak centered at 505 nm (green emission), due to the thickness of the MEH-PPV single layer. Also from Figure 2, it can be observed that the red-orange bands disappear with dose levels, while the green emission (450–650 nm) bands present a substantial increase in intensity. This result is in agreement with the replacement of vinyl groups (C═C) by carbonyl groups (C═O) on the MEH-PPV backbone due to the photoxidation process.[35,36,40] Likewise, it is very important to emphasize that the increase in the intensity of the green emission occurs until a specific dose for each LR/LG value, as shown in Figure 3.

From the results shown in Figures 2 and 3, a strong relation between final color (i.e., saturation color) of the dosimeter for a specific radiation dose and LR/LG parameters can be noted. The relation between them is shown in Figure 4. It is observed that the dose–response of the dosimeter is linearly dependent on the number of DY220 and MEH-PPV layers, thus being a readable way to following the gamma exposure, which might be helpful in order to analyze quality assurance and control of the food irradiation process. Therefore, depending on the LR/LG value, it can be used as a dosimeter and label in radiation processing in the dose range from 0 to 10 kGy.

The effect of gamma radiation dose on the fluorescence of the device is shown in Figure 5. The color coordinates for CIE (1931) chromatic diagram of D_3M_3 and D_3M_4 devices exposed to gamma radiation are shown in Figure 5(a,b), respectively. The results demonstrate the luminescence color variation of the material from red [$x = 0.31$, $y = 0.39$ (D_3M_3) and $x = 0.34$, $y = 0.35$ (D_3M_4)] to green [$x = 0.21$, $y = 0.42$ (D_3M_3) and $x = 0.19$, $y = 0.38$ (D_3M_4)]. These values indicate and emphasize a marked influence of gamma radiation on the emission color of the DY220:MEH-PPV multilayer films, as previously pointed out in Figures 2, 3, and 5.

In order to obtain color comparisons and measurements of color-dose–dependence for the dosimeters developed, Figure 6 shows a standardized color chart for food irradiation management and pictures from the DY220:MEH-PPV multilayer films exposed to high doses of gamma radiation (>0.5 kGy). It should be noted that all pristine devices present a red-orange

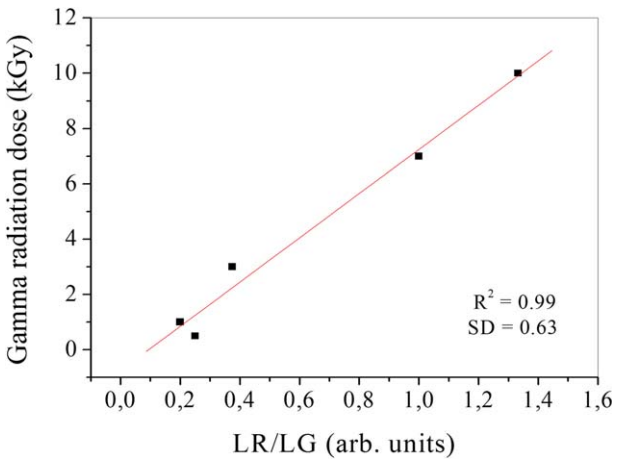

Figure 4. Linear relationship between the gamma radiation dose of the most intense PL (λ_{max}) obtained from the spectra in Figure 2 as a function of the coefficient number of red layers and green layers (LR/LG). Full lines denote the linear regression line. [Color figure can be viewed at wileyonlinelibrary.com]

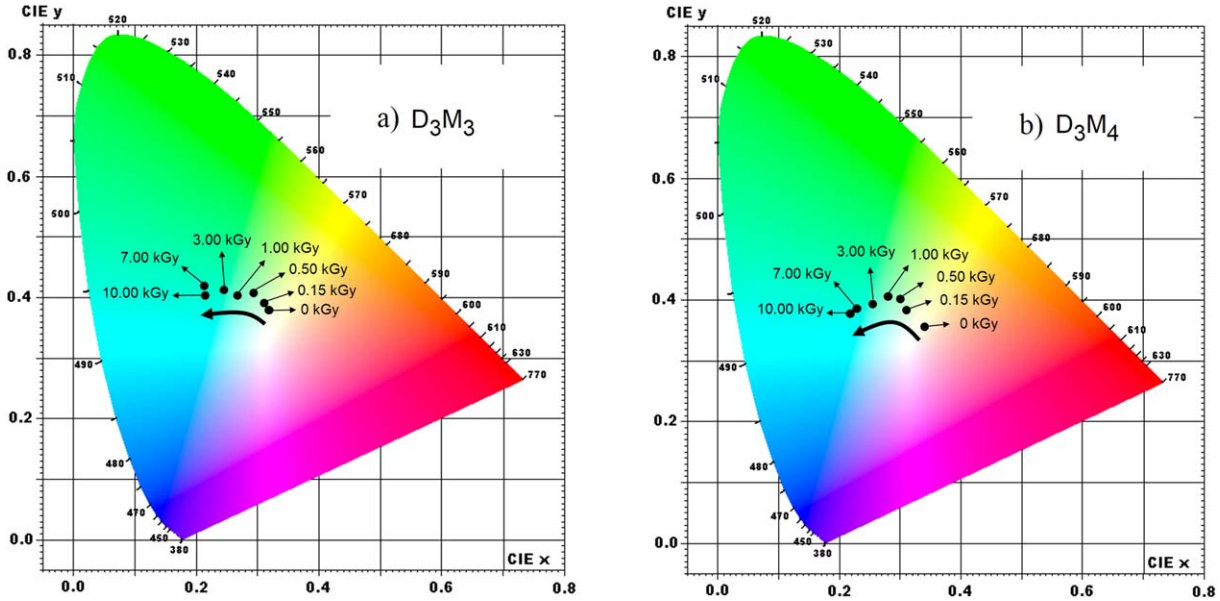

Figure 5. CIE (1931) chromaticity diagram obtained from DY220:MEH-PPV multilayer films exposed to gamma radiation doses equal to 0, 0.15, 0.50, 1.00, 3.00, 7.00, and 10.00 kGy. The diagrams were obtained using the PL spectra shown in (a) Figure 1(d); (b) Figure 1(e); and the Radiant Imaging Color Calculator Free Software. [Color figure can be viewed at wileyonlinelibrary.com]

color, but the color tone changes due to the number or layers of the MEH-PPV film. It can be seen from the color chart that the color of the devices changes to green with radiation exposure.

It is important to observe that the "red-green" color change occurs for a different dose for each device, such as: 0.50 kGy for D_8M_2, 1.00 kGy for D_5M_1, 3.00 kGy for D_8M_3, 7.00 kGy for D_3M_3, and 10.00 kGy for D_3M_4. Consequently, a color chart was easily obtained from the color comparison between the DY220:MEH-PPV dosimeters and a Pantone color code,[45] as shown in Figure 6. By standardizing the color of D_8M_2, D_5M_1, D_8M_3, D_3M_3, and D_5M_4 after they had been exposed to 0, 0.15, 0.50, 1.00, 3.00, 7.00, and 10.00 KGy, a single or a strip dosimeter can be read by visual comparison to the color chart, to take the dose measurement as represented in Figure 7. This result is very important because it shows the possibility of developing versatile dosimeters for different purposes.

It is clear from these results that the rate of the color changes in DY220:MEH-PPV hybrid materials can be altered by manipulating the organic systems, thus allowing the development of dosimeters for a specific gamma radiation dose. In addition, from a review of the materials cost used in the device (paper, DY220, MEH-PPV), it was concluded that the individual value of these devices is <$0.50.

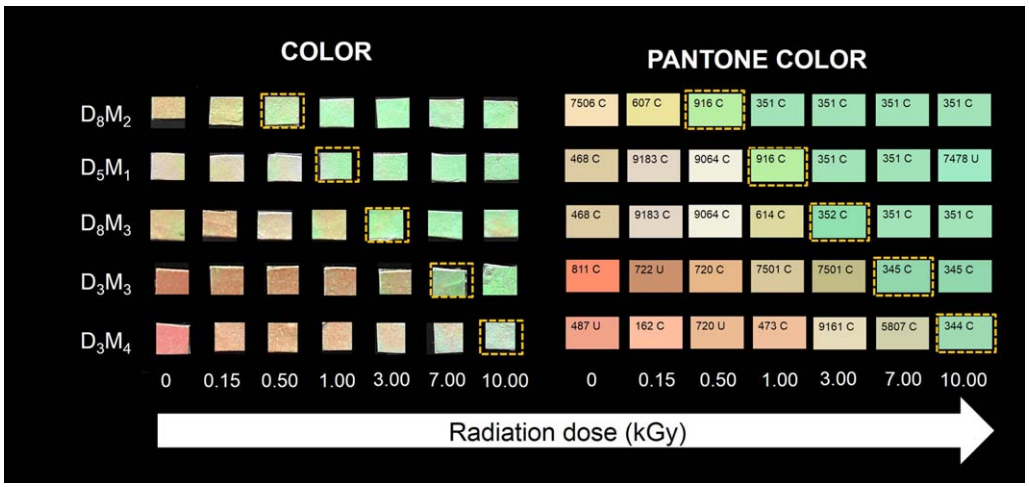

Figure 6. Standardized color chart for gamma radiation based on the color changes of DY220:MEH-PPV multilayer films. On the left, the pictures show the real color change in the devices after exposure to radiation doses equal to 0, 0.15, 0.50, 1.00, 3.00, 7.00, and 10.00 kGy; and on the right, the picture shows the Pantone color code. The dashed lines in the pictures indicate the color of the device when the stipulated dose was reached. [Color figure can be viewed at wileyonlinelibrary.com]

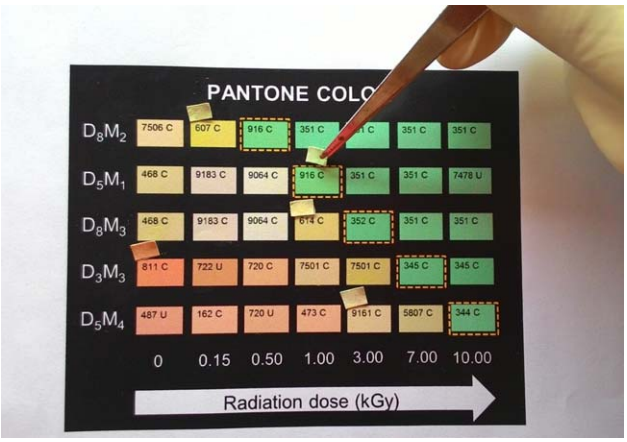

Figure 7. Dosimeter color comparison after irradiation processes against standardized color chart. [Color figure can be viewed at wileyonlinelibrary.com]

CONCLUSIONS

The results reported here clearly demonstrate the feasibility of using DY220:MEH-PPV multilayer film gamma radiation (^{60}Co) dosimeters for a wide dose range. The saturation color of the dosimeters changed linearly as the dose increased, and can be manipulated according to the desired application by changing the number of DY220 and MEH-PPV layers. These results allow for the development of novel color-indicator dosimeters, where red represents underdose and green the dose to be determined. In fact, the $D_{LG}M_{LR}$ structure has been revealed as a multipurpose, easy-to-read, low-cost, user-friendly, and real-time dosimeter for low-medium doses. Additionally, the results support the idea of a novel detector for monitoring, quality assurance and control of food irradiation processes.

ACKNOWLEDGMENTS

The authors would like to thank the Brazilian funding agencies CAPES, CNPq, FAPEMIG, and PRONEM/FAPEMIG, as well as the National Institute of Science and Technology on Organic Electronics (INEO/INCT) for financial support and fellowships.

REFERENCES

1. B. H. M. G. Centro de Desenvolvimento da Tecnologia Nuclear. Brazil, **1991**; p 43.
2. WHO. Geneva, **1981**; p 36.
3. Santos, A. F.; Vizeu, D. M.; Destro, M. T.; Franco, B. D. G. M.; Landgraf, M. *Ciência e Tecnologia De Alimentos.* **2003**, *23*, 200.
4. Podadera, P. Instituto de Pesquisas Energéticas e Nucleares, Autarquia Associada à Universidade de São Paulo, São Paulo, **2007**.
5. Severino, R.; Vu, K. D.; Donsì, F.; Salmieri, S.; Ferrari, G.; Lacroix, M. *J. Food Eng.* **2014**, *124*, 1.
6. Khan, H. M.; Anwer, M.; Chaudhry, Z. S. *Radiat. Phys. Chem.* **2002**, *63*, 713.
7. Kovács, A.; Baranyai, M.; Wojnárovits, L.; Miller, S.; Murphy, M.; McLaughlin, W. L.; Slezsák, I.; Kovács, A. *Radiat. Phys. Chem.* **2002**, *63*, 777.
8. ISO/ASTM International 2013, Switzerland, **2013**; p 6.
9. McLaughlin, W.; Miller, A.; Fidan, S.; Pejtersen, K.; Pedersen, W. B. *Radiat. Phys. Chem.* **1977**, *10*, 119.
10. Buenfil-Burgos, A.; Uribe, R.; De La Piedad, A.; McLaughlin, W.; Miller, A. *Radiat. Phys. Chem.* **1983**, *22*, 325.
11. Miller, A.; Batsberg, W.; Karman, W. *Int. J. Radiat. Appl. Instrum. C. Radiat. Phys. Chem.* **1988**, *31*, 491.
12. Devic, S. *Phys. Med.* **2011**, *27*, 122.
13. Malav, S.; Bera, A.; Tiwari, B.; Prakash, V.; Vaijapurkar, S. *Radiat. Protect. Environ.* **2014**, *37*, 35.
14. Soliman, Y.; Basfar, A.; Msalam, R. *Radiat. Measur.* **2014**, *62*, 45.
15. Abdel-Fattah, A.; Soliman, Y.; Bayomi, A.; Abdel-Khalek, A. *Appl. Radiat. Isot.* **2014**, *86*, 21.
16. Soliman, Y.; Bayomi, A.; Abdel-Fattah, A.; Abdel-Khalek, A. *Sens. Actuator. B: Chem.* **2014**, *200*, 109.
17. Gafar, S.; El-Ahdal, M. *Dyes Pigm.* **2015**, *114*, 273.
18. McLaughlin, W.; Yun-Dong, C.; Soares, C.; Miller, A.; Van Dyk, G.; Lewis, D. *Nucl. Instrum. Methods Phys. Res. Sect. A* **1991**, *302*, 165.
19. Chu, R.; Lewis, D.; O'Hara, K.; Buckland, B.; Dinelle, F.; Van Dyk, G. *Int. J. Radiat. Appl. Instrum. C. Radiat. Phys. Chem.* **1990**, *35*, 767.
20. Vandana, S.; Shaiju, V.; Sharma, S.; Mhatre, S.; Shinde, S.; Chourasiya, G.; Mayya, Y. *Appl. Radiat. Isot.* **2011**, *69*, 130.
21. Lee, S.-R.; Park, J.-Y.; Suh, T.-S.; Park, H.-J.; Lee, J.-W.; Jung, W.-G. *J. Korean Phys. Soc.* **2012**, *61*, 1319.
22. Antar, E.; Gafar, S.; Ahdal, M. E. *Int. J. Low Radiat.* **2014**, *9*, 317.
23. Ebraheem, S.; Beshir, W.; Eid, S.; Sobhy, R.; Kovacs, A. *Radiat. Phys. Chem.* **2003**, *67*, 569.
24. Nilekani, S.; Gupta, B. *Radiat. Phys. Chem.* **2004**, *70*, 697.
25. Khan, H. M.; Naz, S. *Nucl. Sci. Techn.* **2007**, *18*, 141.
26. Khan, H.; Tabassum, S.; Wahid, M. *J. Radioanal. Nucl. Chem.* **2009**, *280*, 635.
27. Khan, H. M.; Naz, S.; Tabassum, S. *J. Radioanal. Nucl. Chem.* **2011**, *289*, 225.
28. Butson, M. J.; Cheung, T.; Yu, P. K. *Australas. Phys. Eng. Sci. Med.* **2004**, *27*, 230.
29. Soares, C. *Radiat. Prot. Dosim.* **2006**, *120*, 100.
30. Muench, P. J.; Meigooni, A. S.; Nath, R.; McLaughlin, W. L. *Med. Phys.* **1991**, *18*, 769.
31. Butson, M. J.; Cheung, T.; Peter, K. *Med. Phys.* **2006**, *33*, 2923.
32. Butson, M. J.; Cheung, T.; Peter, K. *Appl. Radiat. Isot.* **2006**, *64*, 60.
33. Silva, E. A. B.; Borin, J. F.; Nicolucci, P.; Graeff, C. F.; Netto, T. G.; Bianchi, R. F. *Appl. Phys. Lett.* **2005**, *86*, 131902–131902.

34. Ferreira, G. R.; de Vasconcelos, C. K.; Silva, M. M.; dos Santos, F. A.; Pires, J. G.; Duarte, A. S.; Bianchi, A. G. C.; Bianchi, R. F. *MRS Proc.* **2009**, 1209-P1203–1203.

35. Ferreira, G. R.; De Vasconcelos, C. K. B.; Bianchi, R. F. *Med. Phys.* **2009**, *36*, 642.

36. de Vasconcelos, C.; Bianchi, R. *Sens. Actuat. B: Chem.* **2009**, *143*, 30.

37. Schimitberger, T.; Ferreira, G. R.; Saraiva, M. F.; Bianchi, A. G. C.; Bianchi, R. F. *Sens. Actuat. B: Chem.* **2012**, *168*, 131.

38. Schimitberger, T.; Ferreira, G. R.; Souza, C. d J d.; Silva, M. d M.; Saraiva, M. F.; Bianchi, R. F. *Tecnol. Metal. Mater.* **2012**, *9*, 48.

39. Schimitberger, T.; Ferreira, G.; Akcelrud, L.; Saraiva, M.; Bianchi, R. *Med. Eng. Phys.* **2013**, *35*, 140.

40. Bianchi, R. F.; Balogh, D. T.; Tinani, M.; Faria, R. M.; Irene, E. A. *J. Polym. Sci. B: Polym. Phys.* **2004**, *42*, 1033.

41. Liu, J.; Guo, T.-F.; Yang, Y. *J. Appl. Phys.* **2002**, *91*, 1595.

42. Farkas, J.; Mohácsi-Farkas, C. *Trends Food Sci. Technol.* **2011**, *22*, 121.

43. Kim, J.; Moreira, R. G.; Castell-Perez, M. E. *J. Food Eng.* **2015**, *149*, 137.

44. Etienne, J.; Buyle, R. *J. Food Eng.* **1984**, *3*, 265.

45. Available at: http://www.pantone.com/pages/pantone/index.aspx (accessed March 10, **2015**).